Asociación Argentina
de Mecánica Computacional

Mecánica Computacional Vol XXXIX, págs. 983-992 (artículo completo)
F.E. Dotti, M. Febbo, S.P. Machado, M. Saravia, M.A. Storti (Eds.)
Bahía Blanca, 1-4 Noviembre 2022

NUMERICAL ASPECTS IN THE EVALUATION OF TRIGGERING OF STATIC LIQUEFACTION USING THE HSS MODEL

Felipe Lopez Rivarola[a,b], Nicolás Tasso[a,b], Kevin Bernardo[a,b] and Alejo Sfriso[a,b]

[a]*Universidad de Buenos Aires. Facultad de Ingeniería. INTECIN. (UBA-CONICET). flopez@fi.uba.ar*

[b]*SRK Consulting (Argentina),Chile 300, CABA, latam.srk.com*

Keywords: Static Liquefaction, Triggering, Tailing Storage Facilities, Plaxis 2D®, HSS model.

Abstract. Recent failures of upstream-raised Tailings Storage Facilities (TSF) have raised concerns on the stability of these dams, which relies on the strength of tailings, which are loose and normally consolidated rock flour that may exhibit a collapsible structure inducing strong strain-softening in undrained loading. Standard practice to evaluate global stability of TSFs entails the use of limit equilibrium analyses, which consider either peak or residual undrained shear strength. These procedures do not consider the work input required to drive the softening process that leads to progressive failure, and therefore there is room for numerical deformation models to provide further insight of the liquefaction process. This paper describes recent applications of such analyses employing the Hardening Soil Model with Small Strain (HS-Small or HSS) to evaluate triggering of static liquefaction of upstream-raised TSFs. The calibration methodology captures the complete stress path of the softening behavior. The importance of the stiffness parameters that control both the rate of elastic and plastic volumetric strains is disccused. Focus is placed on the parameters of the non-linear solver and their numerical implications. As an example, a TSF is modelled in PLAXIS 2D® to evaluate its vulnerability to static liquefaction due to an undrained lateral spreading at the foundation. It is shown that this procedure is useful to verify the robustness of the TSF design.

1 INTRODUCTION

In mining processing, ore is crushed to rock flour and chemically processed. The waste, tailings, are frequently deposited hydraulically in Tailings Storage Facility (TSF), and not compacted. The combining effect of a loose and saturated state results in a potential for static liquefaction, which implies a sudden loss of strength in undrained shear.

In recent years, the interest on the analysis of tailings static liquefaction has grown due to recent upstream-raised TSFs massive failures -such as Merriespruit, Mount Polley, Samarco and Brumadinho. As a conservative assumption, international guidelines (e.g. ANCOLD (2019)) recommend to assume that static liquefaction will occur on brittle/contractive saturated tailings and to check stability employing residual undrained shear strength. This approach neglects the strains required for the material to reach its residual strength. When such consideration is of value, trigger analyses using deformation modelling is recommended. Trigger analyses assess the stability of equilibrium and the robustness of the system by imposing growing external perturbations until failure is triggered.

In these analyses it is of outmost importance to capture the softening behavior of tailings in undrained shear. An example can be seen in Ledesma et al. (2022), where the authors analyzed the liquefaction vulnerability of tailings dams using the Modified Pastor-Zienkiewicz constitutive model. Although there are several advanced models in the academia that can correctly model softening regime, in the industry these are not commonly used due to difficulties in their implementation or calibration, and lack of industrial robustness of most of them. As an alternative, the Hardening Soil model with Small-strain stiffness (HS-Small or HSS) constitutive model can be calibrated to capture this behaviour using the simplified procedure detailed by Sottile et al. (2021). The methodology uses tools widely available in geotechnical engineering practice for practical static liquefaction assessments.

In this paper the staged construction of a typical TSF and its stability are analyzed. The HSS constitutive model implemented in PLAXIS 2D® is used, and the strategy proposed by Sottile et al. (2021) is followed to overcome the model limitation of not being implemented in a critical state framework. A calibration procedure to capture undrained strength is presented, and the numerical features required are discussed. Special focus is given to the max load fraction per step as small steps are needed to correctly calculate strains and pore pressure, which is essential for trigger analysis. Results from a real TSF are presented and examined as an example.

2 HSS MODEL

HSS is an effective stress, nonlinear elastic, isotropic hardening plasticity model, able to represent the behaviour of materials undergoing plastic compression, consolidation and monotonic shear. The model has two yield surfaces: a shear hardening yield surface, based in Mohr-Coulomb failure criterion, that evolves with plastic shear strain, and a volumetric cap surface that evolves with plastic volumetric and shear strains. The former is used to model plastic strains due to primary deviatoric loading, while the latter is used to model plastic strains due to primary compression in proportional loading, like oedometer or isotropic loading.

When the soil is subjected to drained shear, the relationship between total axial strain and deviatoric stress is approximated by the hyperbolic model (Duncan and Chang, 1970) which is transformed into a hardening rule in the HSS model. Three parameters control the stiffness in shear: at small-strain G_0, in a full unloading-reloading path E_{ur} and the secant stiffness in primary loading at the 50% of the ultimate deviatoric stress E_{50}. All three parameters employ power-law expressions that depend on the minor principal effective stress σ'_3. It should be

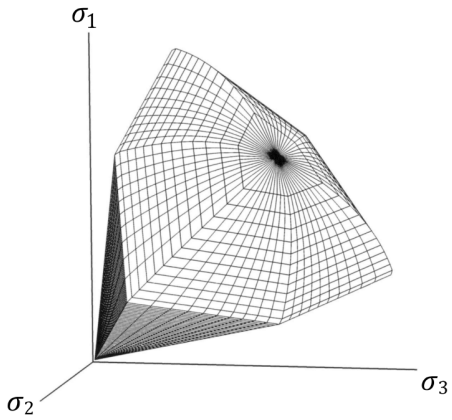

Figure 1: Cap yield and Mohr-Coulomb surfaces of HSS in principal stress for cohesionless soil (PLAXIS®, 2022)

clarified that the stresses are positive for compression in geotechnical practice.

Deformation in proportional compression is controlled by a cap yield surface (Figure 1). Plastic hardening of this yield surface produces both volumetric and shear plastic strain by an associated flow rule. The state variable controlling the position of this yield surface is the isotropic preconsolidation pressure p_p, the parameter controlling its shape is the at-rest stress ratio K_0^{nc} and hardening is controlled by the tangent stiffness E_{oed}, dependent on σ'_3 through a power law.

2.1 Calibration procedure for undrained strength

HSS is a plasticity model that is not implemented in a critical state framework; i.e. the void ratio is not a state variable, so stiffness and strength are independent of void ratio, and a critical state cannot be achieved in drained conditions. This limitation is overcome by using a calibration methodology that focuses on the stiffness parameters that control the rate of shear-induced plastic volumetric strain, such that strain-softening during undrained shearing can be captured (Sottile et al., 2021).

In undrained shear, total volumetric strain increment ε_v is always zero. Decomposition of this strain increment into the elastic and plastic parts yields

$$\varepsilon_v = {\varepsilon_v}^e + {\varepsilon_v}^p = 0 \longrightarrow {\varepsilon_v}^e = -{\varepsilon_v}^p \, . \tag{1}$$

In HSS parameters controlling both strain increments are

$${\varepsilon_v}^e[E_{ur}^{ref}, \nu] = -{\varepsilon_v}^p[E_{50}^{ref}, E_{oed}^{ref}, R_f, \psi] \, , \tag{2}$$

where ν is the Poisson's ratio, R_f the failure ratio of the hyperbolic model and ψ the angle of dilatancy. Adopting $\psi = 0$ and ϕ_{cv}, a stationary condition is achieved

$$\phi_{mob} = \phi_{cv} \longrightarrow \psi_{mob} = 0 \longrightarrow {\varepsilon_v}^p = 0 \, , \tag{3}$$

where the final mobilized friction angle ϕ_{mob} reaches ϕ_{cv} and the final volume and mean effective stress are constant (${\varepsilon_v}^e = -{\varepsilon_v}^p = 0$). This condition is, by definition, the critical state of the material. Calibration of all five parameters E_{ur}^{ref}, ν, E_{50}^{ref}, E_{oed}^{ref}, R_f is then performed to achieve a target peak undrained shear strength ratio $s_u^{peak}/\sigma'_{1,0}$ and a target residual undrained shear strength ratio $s_u^{res}/\sigma'_{1,0}$ at the same time, using a unique set of parameters, and able to performing SHANSEP-type of stability analyses (Ladd and DeGroot, 2003).

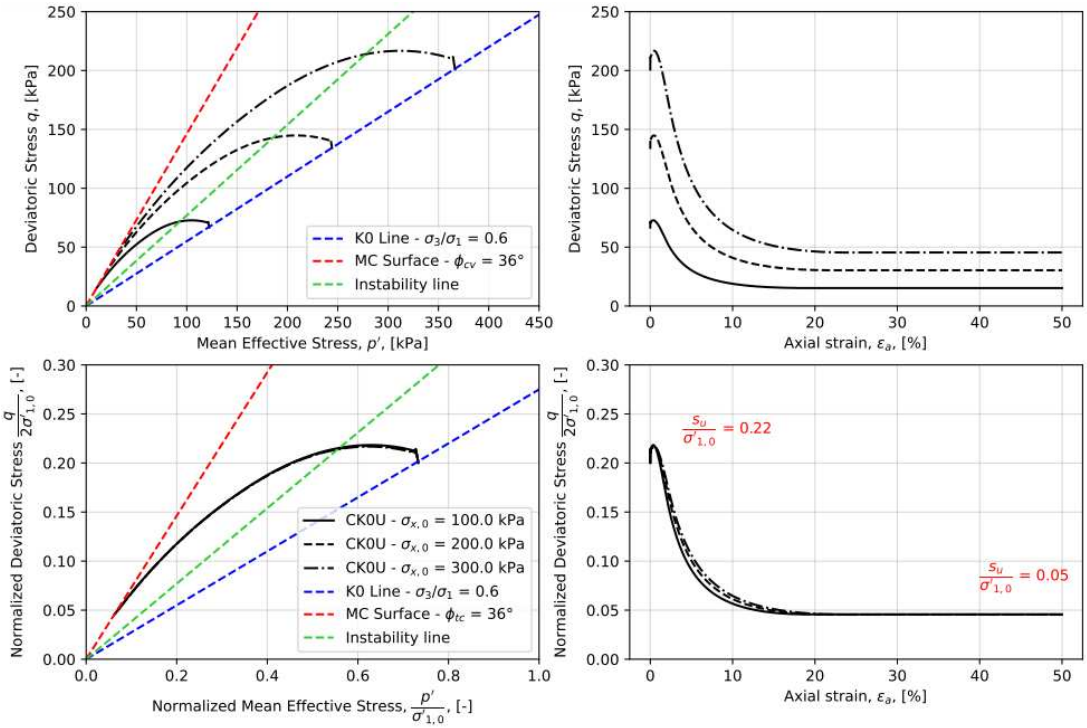

Figure 2: Example of calibration of HSS to reproduce target $s_u^{peak}/\sigma'_{1,0}$ and $s_u^{res}/\sigma'_{1,0}$ ratios, using a unique set of parameters.

Figure 2 shows an example of such calibration. Note that K0-Consolidated Undrained triaxial tests (CK0U) were simulated at three different confining pressures, and the three numerical tests yielded the same peak and residual shear strength ratios. It is important to note the position of the so-called Instability line, which is the line joining the peak values in the p-q diagram.

The typical calibration sequence is:

- calibrate material parameters for drained shear, imposing $\phi = \phi_{cv}$ and $\psi = 0$;
- reduce the ratio E_{50}^{ref} / E_{ur}^{ref} and/or increase ν until a target $s_u^{peak}/\sigma'_{1,0}$ is obtained;
- change R_f until a target $s_u^{res}/\sigma'_{1,0}$ is obtained.

Figure 3 shows the influence of these parameters on the stress-strain curves. Material parameters presented in Table 1 were considered as base parameters.

2.2 Material parameters calibration

As an example, the HSS material model was calibrated following the calibration sequence previously described to represent typical peak and residual undrained shear stress ratios for loose tailings (Been and Jefferies, 1985). Table 1 shows the parameters used, and Figure 4 shows simulations of Direct Simple Shear tests (DSS), which are commonly used to measure the undrained shear stress ratio of soils.

3 NUMERICAL ASSESSMENT OF A TSF

3.1 Model description

An upstream-raised TSF was modelled in PLAXIS 2D® (2021) to evaluate its vulnerability against static liquefaction. The model has 14048 15-node triangular elements and entails five

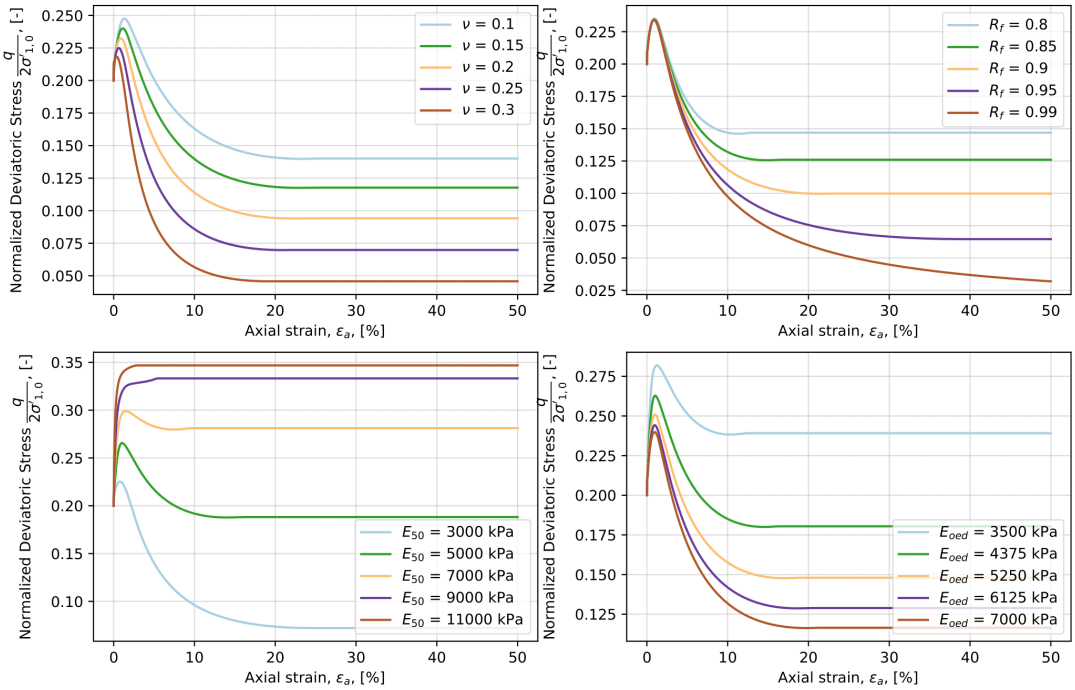

Figure 3: Influence of E_{50}^{ref}, E_{oed}^{ref}, ν and R_f on stress-strain curves and considering the base parameters shown in Table 1.

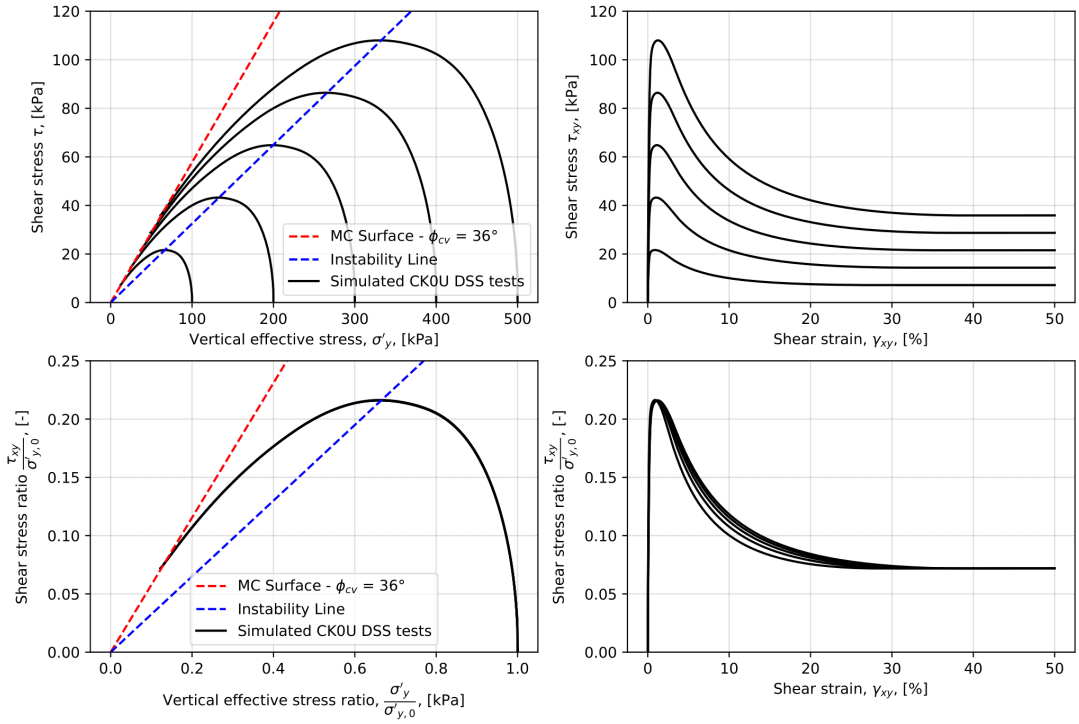

Figure 4: Direct Simple Shear tests (DSS) simulations using parameters of Table 1.

Material parameter	Symbol	Unit	Value
Secant stiffness in standard drained triaxial test	E_{50}^{ref}	MPa	3.4
Tangent stiffness for primary oedometer loading	E_{oed}^{ref}	MPa	9.0
Unloading/reloading stiffness from drained triaxial test	E_{ur}^{ref}	MPa	60
Power of stress-level dependency of stiffness	m	-	0.80
Poisson's ratio for unloading/reloading	ν_{ur}	-	0.30
K_0-value for normal consolidation	K_0^{nc}	-	0.60
Reference stress for stiffness	p_{ref}	kPa	100
Reference shear modulus at very small strain ($\varepsilon < 10^{-6}$)	G_0^{ref}	MPa	50
Threshold shear strain at which $G_s = 0.722G_0$	γ_{07}	$\%$	0.01
Effective cohesion	c'_{ref}	kPa	0
Effective angle of internal friction	ϕ_{cv}	^{o}	36
Angle of dilatancy	ψ	^{o}	0
Failure ratio	R_f	-	0.90

Table 1: HSS Material parameters used, calibrated for a tailings material.

geotechnical units: tailings, embankment raises, buttress, starter wall and bedrock. The geometry and mesh are presented in Figure 5, and the quality check is shown in Figure 6. The embankment raises, tailings, starter wall and buttress were modelled using HSS and the bedrock as linear elastic; parameters are shown in Table 2.

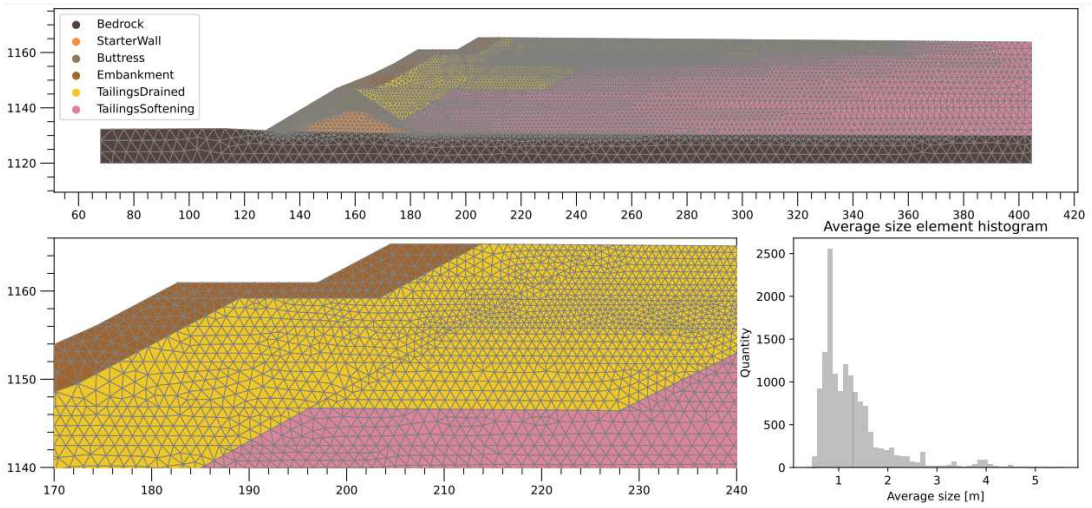

Figure 5: Upper and left: Model geometry and mesh. Right: Average size elements histogram.

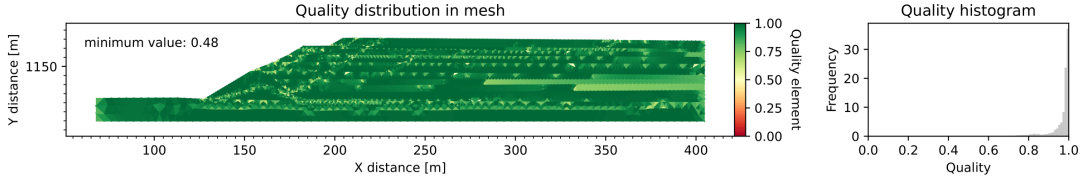

Figure 6: Left: Quality distribution in mesh. Right: Quality histogram.

Parameter	Unit	Tailings	Embankment	Buttress	Starter Wall	Bedrock
$\gamma unsat$	kN/m^3	21	21	21	20	24.4
γsat	kN/m^3	22	22	22	21	24.5
E_{50}^{ref}	MPa	4	4	20	40	-
E_{oed}^{ref}	MPa	3.5	3.5	16	32	-
E_{ur}^{ref}	MPa	50	50	60	120	-
m	-	0.80	0.80	0.50	0.5	-
ν_{ur}	-	0.30	0.30	0.20	0.20	-
K_0^{nc}	-	0.60	0.60	0.50	0.50	-
p_{ref}	kPa	100	100	100	100	-
G_0^{ref}	MPa	80	80	100	200	-
γ_{07}	%	0.01	0.01	0.01	0.01	-
c'_{ref}	kPa	0	2	2	0	-
ϕ_{cv}	^{o}	36	36	37	33	-
ψ	^{o}	0	0	0	0	-
R_f	-	0.90	0.90	0.90	0.90	-
E	GPa	-	-	-	-	10.8
ν	-	-	-	-	-	0.20

Table 2: Material parameters used, calibrated for tailings, embankment, buttress, starter wall and bedrock.

3.2 Model strategy

The TSF was raised in several stages until its current configuration is reached, using an average raise height of 3.0 m and an average rate of rise of 2 m/year. The aim is to reasonable capture the staged construction process and its associated non-linearities that determine the in-situ stress field and pore pressure distribution. A steady state groundwater flow is computed at each raise, while excess pore pressures are generated due to the tailings raise itself; thus, a decoupled flow-deformation scheme was adopted.

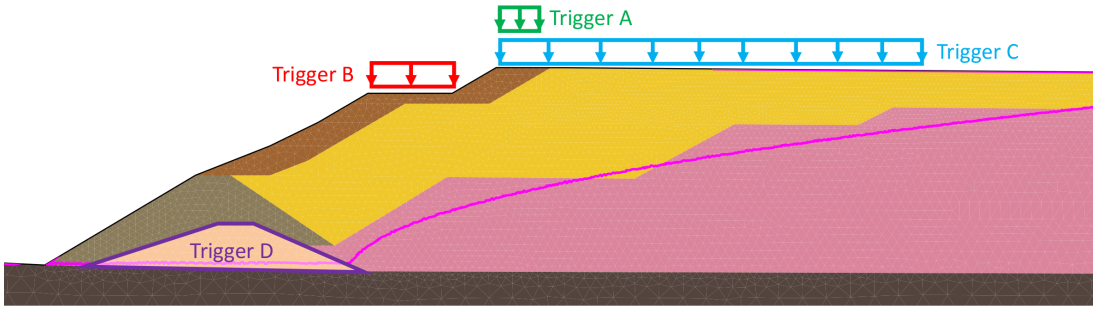

Figure 7: Triggers applied to the model.

Once the current TSF condition was reached, flow liquefaction triggers were analyzed. Typical triggers are: instant loads at various places in the crest; deformations at the foundation or starter embankment inducing shear in the tailings body; raise in the phreatic surface, or surface water inflow; spontaneous liquefaction of a small cluster within the tailings body. In this paper, four triggers were analysed (Figure 7): three loads at different locations (triggers A, B, and C) and a deformation at the foundation (trigger D).

Triggers A and B apply a load at the current dam crest and the berm, respectively; this aims

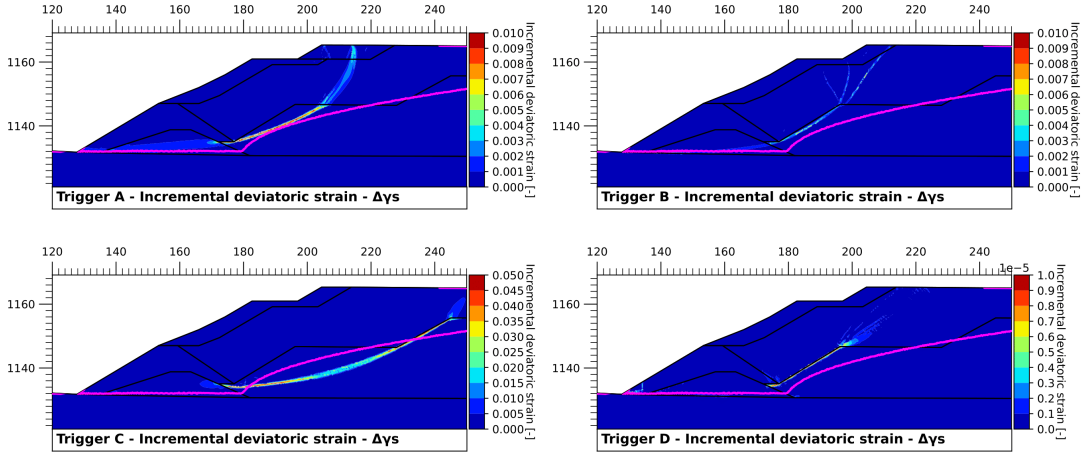

Figure 8: Incremental deviatoric strain contour maps.

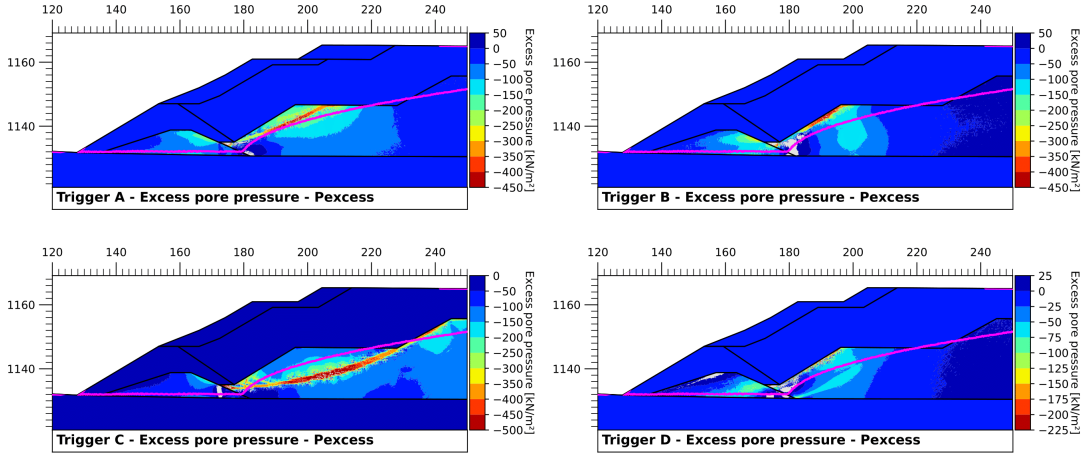

Figure 9: Excess pore pressure contour maps.

to represent heavy traffic loads or stockpiled material during regular mine operation. Trigger C was applied along the full tailings surface to represent a rapid raise on the tailings level. Trigger D applies a contraction -by means of a horizontal strain- at the toe of the upstream embankment raises; this aims to represent eventual movements due to an accidental excavation during the buttress construction or a sudden loss/collapse of material due to piping.

It must be mentioned that all the trigger analyses were done considering an undrained behavior of the tailings material in the saturated region (i.e. nil volumetric strains with subsequent excess pore pressures generation during shearing).

3.3 Results: Failure surfaces

The failure surfaces are shown in Figure 8 where the incremental deviatoric strains are plotted. All triggers generate a global failure due to the progressive buildup of pore pressure, see Figure 9, demonstrating that the failure surface coincides with the highest pore pressure, as this is what generates the drop in the effective stress which leads to static liquefaction. Finally, in Figure 10 points where the stress state is above the instability line is shown. It can be seen that what triggers failure is not the amount of tailings above the instability line but if the material above the instability line forms a chain that generates a kinematically admissible failure surface.

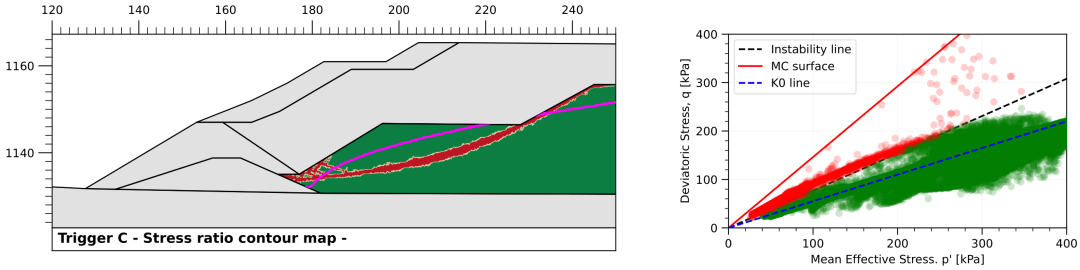

Figure 10: Right: stress state of every stress point of tailings material showed in a p-q plot. Left: Stress points whose stress state is above the instability line.

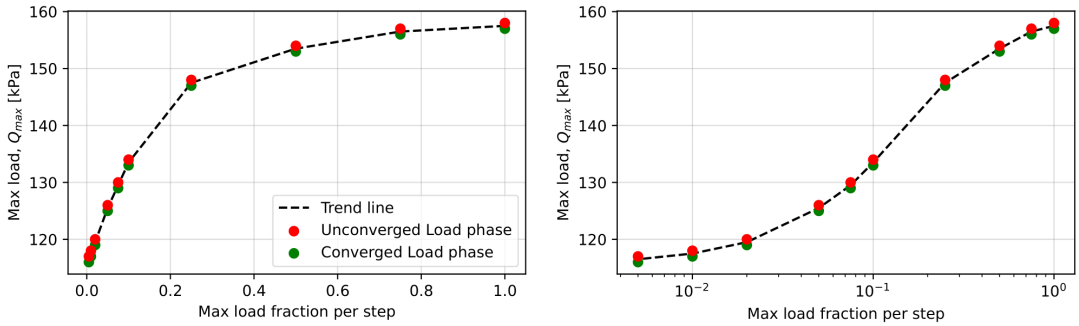

Figure 11: Influence of max load fraction per step on maximum load of trigger B.

3.4 Results: Step size

As previously discussed, when doing undrained analysis there is no total volumetric strain but there are both plastic and elastic strains ($\varepsilon_v = 0$ but ${\varepsilon_v}^e = -{\varepsilon_v}^p \neq 0$). Hence, in trigger analysis, even if the total strain remains small, there may be (and frequently are) large plastic and elastic strain increments. Plaxis solver controls total displacements, and thus total strain increments. As the plastic and elastic strains of the trigger phase can be large, and these are responsible for the excess pore pressure that leads to undrained softening, using default numerical parameters can result in inaccurate pore pressure and trigger loads. This leads to a need to force smaller steps in order to correctly calculate the strains by controlling the max load fraction per step (*mlfps*). The problem is illustrated in Figure 11, where data points were computed in the model provided above for trigger B. As it can be seen, as the *mlfps* was reduced so does the trigger load, but it converges to a fixed value with small enough step size. Table 3 shows the trigger values (maximum load or strain) using a *mlfps* of 0.5 and 0.01 for the four triggers analyzed. In this example a difference of up to 30% can be found, but value up to 100% were found in other cases.

Trigger	Description	Trigger for *mlfps* 0.5	Trigger for *mlfps* 0.01	Increment
A	Load at the crest	332 kPa	310 kPa	7,1 $\%$
B	Load at the berm	153 kPa	117 kPa	30,7 $\%$
C	Beach load	120 kPa	107 kPa	12.5 $\%$
D	Contraction	1.0 $\%$	1.0 $\%$	-

Table 3: Trigger values for different max load fraction per step.

4 CONCLUSIONS

In this paper the application of Hardening Soil Model with Small Strain to evaluate triggering of static liquefaction of an upstream-raised TSF were discussed. The strategy proposed by Sottile et al. (2021) was followed. A calibration procedure to capture undrained strength was presented, and the numerical features required were discussed. Focus was given to the parameters of the non-linear solver and their numerical implications. As an example, a TSF was modelled in PLAXIS 2D® to evaluate its vulnerability to static liquefaction due to an undrained lateral spreading at the foundation. The importance of the role of pore pressure calculation was discussed. It was shown that the procedure used is useful to verify the robustness of the TSF design, but special attention must be given to the max load fraction per step used. A lower value than the default must be used to ensure that strains and pore pressure increment are correctly calculated.

REFERENCES

ANCOLD. *Guidelines on tailings dams - Planning, design, construction, operation and closure - revision 1*, 2019.

Been K. and Jefferies M.G. A state parameter for sands. *Géotechnique*, 35:99–112, 1985.

Duncan J.M. and Chang C.Y. Nonliner analysis of stress and strain in soil. *ASCE Journal of the Soil Mechanics and Foundation*, pages 1629–1653, 1970.

Ladd C.C. and DeGroot D.D. Recommended practice for soft ground site characterization: Arthur casagrande lecture. *Arthur Casagrande Lecture, 12th Panamerican Conference on Soil Mechanics and Geotechnical Engineering*, 2003.

Ledesma O., Sfriso A., and Manzanal D. Procedure for assessing the liquefaction vulnerability of tailings dams. *Computers and Geotechnics*, 144:104–632, 2022. ISSN 0266-352X. doi: https://doi.org/10.1016/j.compgeo.2022.104632.

PLAXIS®. Material models manual - connect edition v22.01. *Bentley*, 2022.

Sottile M.G., Cueto I.A., Sfriso A.O., Ledesma O.N., and Lizcano A. Flow liquefaction triggering analyses of a tailings storage facility by means of a simplified numerical procedure. *Proceedings of the 20th International Conference on Soil Mechanics and Geotechnical Engineering*, 2021.